

Major histocompatibility complex-class II is induced by Interferon-gamma and follows three distinct patterns of expression in colorectal cancer organoids

Pickles, Oliver J; Wanigasooriya, Kasun; Ptasinska, Anetta; Patel, Akshay J.; Robbins, Helen L; Bryer, Claire; Whalley, Celina M; Tee, Louise; Lal, Neeraj; Pinna, Maria; Elzefzafy, Nahla; Taniere, Philippe; Beggs, Andrew D; Middleton, Gary M.

DOI:

[10.1158/2767-9764.CRC-23-0091](https://doi.org/10.1158/2767-9764.CRC-23-0091)

License:

Creative Commons: Attribution (CC BY)

Document Version

Publisher's PDF, also known as Version of record

Citation for published version (Harvard):

Pickles, OJ, Wanigasooriya, K, Ptasinska, A, Patel, AJ, Robbins, HL, Bryer, C, Whalley, CM, Tee, L, Lal, N, Pinna, M, Elzefzafy, N, Taniere, P, Beggs, AD & Middleton, GM 2023, 'Major histocompatibility complex-class II is induced by Interferon-gamma and follows three distinct patterns of expression in colorectal cancer organoids', *Cancer Research Communications*. <https://doi.org/10.1158/2767-9764.CRC-23-0091>

[Link to publication on Research at Birmingham portal](#)

General rights

Unless a licence is specified above, all rights (including copyright and moral rights) in this document are retained by the authors and/or the copyright holders. The express permission of the copyright holder must be obtained for any use of this material other than for purposes permitted by law.

- Users may freely distribute the URL that is used to identify this publication.
- Users may download and/or print one copy of the publication from the University of Birmingham research portal for the purpose of private study or non-commercial research.
- User may use extracts from the document in line with the concept of 'fair dealing' under the Copyright, Designs and Patents Act 1988 (?)
- Users may not further distribute the material nor use it for the purposes of commercial gain.

Where a licence is displayed above, please note the terms and conditions of the licence govern your use of this document.

When citing, please reference the published version.

Take down policy

While the University of Birmingham exercises care and attention in making items available there are rare occasions when an item has been uploaded in error or has been deemed to be commercially or otherwise sensitive.

If you believe that this is the case for this document, please contact UBIRA@lists.bham.ac.uk providing details and we will remove access to the work immediately and investigate.

Download date: 26. Aug. 2023

Major histocompatibility complex-class II is induced by Interferon-gamma and follows three distinct patterns of expression in colorectal cancer organoids

Authors: Oliver J Pickles^{1,3}, Kasun Wanigasooriya², Anetta Ptasinska², Akshay J Patel^{1,3}, Helen L Robbins¹, Claire Bryer², Celina M Whalley², Louise Tee², Neeraj Lal², Maria Pinna², Nahla Elzefzafy^{2,4}, Philippe Taniere³, Andrew D Beggs^{2,3}, Gary M Middleton^{1,3}.

1. Institute of Immunology and Immunotherapy, College of Medical and Dental Science, University of Birmingham, Vincent Drive, Edgbaston, Birmingham, B15 2TT, UK.
2. Institute of Cancer and Genomic Science, College of Medical and Dental Science, University of Birmingham, Vincent Drive, Edgbaston, Birmingham, B15 2TT, UK.
3. University Hospitals Birmingham NHS Foundation Trust, Birmingham, B15 2WB, UK.
4. Cancer Biology department, National Cancer Institute, Cairo University, Cairo, 11796, Egypt.

Correspondence: Prof Gary Middleton, Institute of Immunology and Immunotherapy, College of Medical and Dental Science, University of Birmingham, Vincent Drive, Edgbaston, Birmingham, B15 2TT, UK. Email: g.middleton@bham.ac.uk Telephone: +44 (0) 121 414 7144. Fax +44 (0) 121 414 4486.

Running Title: MHC-Class II regulation in CRC organoids

Keywords: Colorectal cancer, HLA Class II Alleles, Antigen Presentation, Microsatellite Instability, Methylation

Acknowledgments/Financial Support: This work was funded by a Cancer Research UK Clinical Research Training Fellowship (C17422/A25154) awarded to OJP. ADB was funded by a Cancer Research UK Advanced Clinician Scientist award (ref C31641/A23923). NL is supported by a NIHR Clinical Lectureship award.

Conflicts of interest: The authors declare no potential conflicts of interest

Word Count: 5209. 6 Figures, 2 tables.

Contributors: OJP, ADB and GWM conceived the project design. OJP, KW, MP performed organoid development and culture; OJP and AP performed ChIP experiments; AJP, ADB, CB and CMW performed sequencing and analysis; OJP, CMW and LT performed pyrosequencing and RT-qPCR; NL performed TCGA analysis; OJP, HLR and NE performed Western Blots; PT performed IHC; OJP, NL and NE performed flow cytometry. Data analysis performed by OJP, ADB and GWM. Manuscript written by OJP and GYM. All authors reviewed and approved the final manuscript.

Abstract

Tumor-specific MHC class II (tsMHC-II) expression impacts tumor microenvironmental immunity. tsMHC-II positive cancer cells may act as surrogate antigen-presenting cells and targets for CD4+ T cell-mediated lysis. In colorectal cancer (CRC) tsMHC-II negativity is common, in cell lines due to *CIITA* promoter methylation. To clarify mechanisms of tsMHC-II repression in CRC, we analysed CRC organoids which are epigenetically faithful to tissue of origin. 15 primary CRC organoids were treated with IFN γ +/- epigenetic modifiers: flow cytometry was used for tsMHC-II expression. RT-qPCR, total RNAseq, nanopore sequencing, bisulfite conversion/pyrosequencing and western blotting was used to quantitate *CIITA*, STAT1, IRF1 and JAK1 expression, mutations and promoter methylation and ChIP to quantitate H3K9ac, H3K9Me2 and EZH2 occupancy at *CIITA*.

We define three types of response to IFN γ in CRC: strong-, weak- and non-inducibility. Delayed and restricted expression even with prolonged IFN γ exposure was due to IFN γ -mediated EZH2 occupancy at *CIITA*. tsMHC-II expression was enhanced by EZH2 and HDAC inhibition in the weakly inducible organoids. Non-inducibility is seen in three CMS1 organoids due to JAK1 mutation. No organoid demonstrates *CIITA* promoter methylation. Providing IFN γ signalling is intact, most CRC organoids are class II inducible. Upregulation of tsMHC-II through targeted epigenetic therapy is seen in 1/15 organoid. Our approach can serve as a blueprint for investigating the heterogeneity of specific epigenetic mechanisms of immune suppression across individual patients in other cancers and how these might be targeted to inform the conduct of future trials of epigenetic therapies as immune adjuvants more strategically in cancer.

Significance Statement:

Cancer cell expression of MHC class II significantly impacts tumor microenvironmental immunity. Previous studies investigating mechanisms of repression of IFN γ -inducible class II expression using cell lines demonstrate epigenetic silencing of interferon pathway genes as a frequent immune evasion strategy. Unlike cell lines, patient-derived organoids maintain epigenetic fidelity to tissue of origin. In the first such study, we analyse patterns, dynamics and epigenetic control of IFN γ -induced class II expression in a series of colorectal cancer organoids.

Introduction

The absence of tumor-specific MHC class II expression (tsMHC-II) is seen in around 50% of proficient mismatch repair (pMMR) colorectal cancer (CRC) and just under 30% of dMMR CRC and is associated with poor prognosis.(1) Most epithelial cells do not constitutively express class II but can be induced to do so by IFN γ , which transcriptionally activates promoter IV of the class II master transcriptional activator (CIITA_{IV}). Multiple studies have demonstrated that many cancer cell lines are not class II inducible by IFN γ due to transcriptional silencing of *CIITA*.(2-5) In cell lines, this involves *CIITA* promoter CpG methylation with accompanying deficient histone H3 acetylation and high H3K9 methylation upon IFN γ treatment.(2)

tsMHC-II has a profound impact on anti-cancer immunity. *CIITA*-transfected cancer cells are readily rejected unlike their class II negative counterparts and massively infiltrated by immune effector cells.(6-8) Rejection is eliminated in IFN γ knockout mice. CD4⁺ T cell depletion reduces the number of activated CD8⁺ T cells and abrogates the protective effect of cancer cell class II expression. CD4⁺ T cell help for CD8⁺ T cells is crucial in the generation of robust effector and memory CTL responses(9): immunological protection of *CIITA* transfected cells is due to the generation of primed CD4⁺ T cells providing help for the generation of cancer antigen-specific CTL effectors.(7, 10) Importantly, *CIITA* transfected cells function as surrogate APCs priming naïve T cells in the absence of dendritic cells (DCs) and other antigen-presenting cells (APCs).(8) Unmanipulated colonic epithelial cells can take up antigen, present this to antigen-specific CD4⁺ T cells and activate them in a class II restricted manner.(11, 12) Surrogate APCs have the theoretical advantage over DCs in that they can present endogenously processed class II mutated neo-antigens alongside endocytosed antigen from dying cancer cells.(13)

Transfection studies involve cells with forced high-level expression, but importantly IFN γ -induced tsMHC-II also drives enhanced immunity. A recent study compared two orthotopic immunocompetent mouse models of lung cancer, one sensitive to anti-PD-1 (CMT167) and one resistant (LLC). MHC-II is not constitutively expressed on CMT167 cells but can be induced by IFN γ but cannot be induced by IFN γ on LLC cells. *In vivo* CIITA knockdown in CMT167 significantly reduces microenvironmental Th1 immunity, CD8⁺ cell number and reduced efficacy of anti-PD-1 therapy.(14). In bladder cancer, CD4⁺ TILs are directly cytotoxic for autologous cancer cells and CD4⁺ T effectors recognise antigen on cancer cells in a class II-dependent fashion.(15) Intratumoral CD4⁺ T cells correlate with anti-PD-L1 efficacy. Direct CD4⁺ T cell mediated cytolysis of melanoma cells has been described.(16)

Given this pro-immune impact of tsMHC-II expression, one of the immunological escape mechanisms that CRC cells might utilise is cell-autonomous transcriptional repression of *CIITA* and consequent non-inducibility of tsMHC-II by IFN γ . Absence of tsMHC-II may be particularly relevant in CRC due to the low abundance of cDC1,(17) in part related to Wnt signalling,(18) which reduces intra-tumoral recruitment of cDC1.(19) Mice with class II negative cDC1 show weak expansion of antigen-specific CD8⁺ cells and fail to reject tumors, indicating that class II on cDC1 (the paradigmatic professional APC) is required to mediate tumor regression.(20)

These studies suggest that strategies to augment tsMHC-II inducibility could improve the impact of checkpoint blockade in CRC. Given the aforementioned cell line data, the addition of DNA methyltransferase inhibitors would appear to be a reasonable approach, particularly in tsMHC-II negative CRC and given that DNMT inhibition alone can reverse the inhibitory histone marks of deacetylated histone H3 and methylated H3K9.(21) However, the use of cell lines to investigate the epigenetic status of genes, such as *CIITA*, is problematic. CpG island hypermethylation is significantly increased in cancer cell lines compared with corresponding primary tissues,(22) an effect particularly observed in CRC.(23) Organoids are self-organising 3D structures that better model *in vivo* morphologies and cell-cell contacts. Importantly over prolonged periods in culture (up to three months), intestinal epithelial organoids stably maintain the specific promoter methylation profile of the gut region from which they are derived, with recent data importantly demonstrating fidelity of methylation patterns specifically in CRC organoids.(24, 25) Organoids are thus a more appropriate model to interrogate patterns of DNA methylation in colorectal cancer.

We present an analysis of tsMHC-II inducibility in a series of fifteen CRC organoids, focusing on the cancer cell-autonomous mechanisms restricting Class II expression via *in vitro* IFN γ stimulation. Although there are other triggers of tsMHC-II induction, IFN γ is of particular importance. The sensing by DCs of IFN γ produced by tumour-infiltrating T cells is critical to the response to anti-PD-1. IFN γ blockade abrogates tumour control by anti-PD-1 and alongside the resulting DC-produced IL-12, underlies effective immune checkpoint blockade.(26) The rejection of *CIITA*-transfected cells is eliminated in IFN γ knockout mice.(7) Additionally, our approach allows us to map the *in vitro* results to the microenvironmental characteristics of the cancer tissue from which the organoids are derived, something which is not possible with commercially obtained cell lines. The principal aim of this study is to understand the role, if any, of epigenetic mechanisms in silencing inducible tsMHC-II in CRC and thus guide potential therapeutic exploitation utilising epigenetic modifiers. Such an approach, in combination with immune checkpoint blockade, could harness CRC cells as surrogate APCs and generate cancer cells as direct targets for CD4⁺ T cells and improve the effectiveness of immunotherapy in tumors such as pMMR CRC.

Methods

Organoid, 2D Cell Culture and IHC

All patients were recruited at University Hospitals Birmingham NHS Foundation Trust. Patients were formally consented and ethical approval (North West-Haydock Research Ethics Committee Ref 15/NW/0079, sub-approval 17-287). Organoids were derived from representative primary tumor samples. Protocols as originally described by the Hubrecht Organoid Technology (HUB)/Clevers lab were followed.(27, 28) Samples were washed and broken down with tissue processing scissors in tumor digestion buffer,(28) filtered and suspended in Matrigel (Corning, USA). Intesticult Human Organoid growth media (Stemcell Technologies, Canada) supplemented with Primocin antimicrobial (Invivogen, France) was added to wells and plates maintained in a humidified incubator at 37°C with 5% CO₂. Rho kinase inhibitors (Y-27632; Stratech, UK) were used during initial derivation and freeze/thawing steps. For passaging and experimental use, organoids were separated from Matrigel using organoid harvesting solution (Bio-Techne, USA) and a combination of mechanical and chemical digestion with TrypLE Express (Gibco, Denmark). Three organoid

models (COLO151, COLO155 and COLO312) were derived by the Wellcome Trust Sanger Institute as part of the Human Cancer Models Initiative Programme.

2D cell lines including HCT116 (Horizon Discovery, UK, RRID:CVCL_0291), RKO (AMS Biotechnology Europe Ltd, UK, RRID:CVCL_0504), HT29 (ATCC, RRID:CVCL_0320) and DLD1 (ATCC, RRID:CVCL_0248) were obtained directly from the cell banks (supplier confirmed mycoplasma and STR integrity) as listed above. Lines used for experiments were fresh from supply/resuscitation (< 3 months and < 10 passages) and were grown in dedicated 2D culture facilities and media conditions as routinely described. Cell lines and organoids were regularly tested (every 1-2 months) for the presence of mycoplasma infection with the EZ-PCR Mycoplasma Test Kit (Biological Industries, Israel). Details of previously described 2D cell line Class II inducibility and CIITA^{pIV} methylation status(2) and characteristics of lines(29) summarised in Supplementary Table 1.

Tumor FFPE sections were sent for Immunoscore performed by HaliDx (France). Primary tumor IHC staining for class II was performed using an anti-HLA DR,DP,DQ antibody (CR3/43, ab17101; Abcam, UK, RRID:AB_443647) which has been previously validated for use in a clinical trial (ANICCA-Class II). At least two sections from each tumor were sent for blind scoring by a Consultant Pathologist.

Interferon and drug experiments

Interferon stimulation was performed on whole organoid cultures, three days after plating to allow organoid formation. Interferon-gamma (IFN γ) was purchased from Stratech Scientific (UK). A dose of 75 IU/ml was selected based on maximal pathway activation (IRF1/STAT1 expression on western blot) and no incremental increase in class II positive cells (flow cytometry) observed with higher doses. GSK126 (direct selective EZH2 inhibitor) and entinostat (HDAC inhibitor) were purchased from Stratech Scientific (UK) and 5-Azacytidine (DNA methyltransferase inhibitor) from Generon (UK). Cell viability readouts for organoids were performed using the CellTiter-Glo 3D Cell Viability Assay (Promega, USA) and controlled using an ATP standard curve.

Western blots

Cells were lysed in RIPA buffer (Thermo Scientific, USA) with 1x Protease/Phosphatase inhibitor cocktail (Cell Signalling Technology, USA). Quantified protein was loaded onto Mini-PROTEAN TXG Precast Gels (Bio-Rad, USA) and resolved using SDS-PAGE and wet transfer onto PVDF membranes. Membranes were probed with the following primary antibodies (see also dilutions, catalogue number and where available clone numbers): STAT1 (1:1000, #9175, 42H3, Cell Signalling Technology/CST, RRID:AB_2197984), IRF1 (1:1000, #GTX129134, Source Bioscience, RRID:AB_2885905), Jak1 (1:1000, #29261, E3A6M, CST, RRID:AB_2798972), GAPDH (1:1000, #5174, D16H11, CST, RRID:AB_10622025). Blots were developed using chemiluminescence with digital capture of images performed using a Fusion FX6XT digital imaging system (Vilber Lourmat, Germany).

Flow cytometry

Organoids were dissociated into single cells. Staining with eBioscience Fixable Viability Dye eFluor 780 (ThermoFisher Scientific, USA) followed by fluorophore-conjugated antibodies was performed. The following antibodies and dilutions were used: HLA-A,B,C (1:100, APC-

conjugated, W6/32, Biolegend, RRID:AB_314879), HLA-DR,DP,DQ (3:100, PE-Cy7-conjugated, Tü39, Biolegend, RRID:AB_2564279). Gating for singlets, cells and live cells was performed and fluorescence minus one controls were used for class II, with gating strategy displayed in Figure 1. Each experiment was performed in minimum of triplicate with comparison of stimulated and control cells under each condition. Cells were analysed using a LSR Fortessa X-20 flow cytometer (BD), with data analysis performed using FlowJo (Version 10.5.3, BD). Compensation of data was performed in FlowJo with single-stained UltraComp eBeads (ThermoFisher, USA).

DNA/RNA isolation and *CIITA* Quantitative reverse transcription PCR (RT-qPCR), total RNA sequencing, whole genome sequencing and nanopore sequencing

DNA and RNA were isolated from cultures using the AllPrep DNA/RNA kit (QIAGEN, Germany). DNase treatment of RNA was performed utilising the TURBO DNA-free kit (ThermoFisher Scientific, Lithuania), followed by synthesis of cDNA using the High-Capacity RNA-to-cDNA kit (ThermoFisher Scientific, Lithuania). *CIITA* and housekeeping (*GAPDH*) mRNA expression was assessed using a TaqMan fast-cycling protocol on a Quantstudio 5 using ThermoFisher TaqMan Gene Expression arrays for *CIITA* (Hs00172106_m1) and *GAPDH* (Hs02786624_g1). Reaction was performed in quadruple for each gene and +/- IFN γ , with relative increase in *CIITA* expression calculated using the $2^{-\Delta\Delta Ct}$ method.

Total RNA sequencing was performed after ribo-depletion with the NEBNext Ultra II Directional RNA Library Prep Kit for Illumina (New England BioLabs, USA). Libraries were pooled before running on the Illumina NextSeq500 platform with 75bp paired-end reads. The normalized read count data for all expressed coding transcripts was processed by DESeq2 (v.4.0.2) software. A cut-off of gene-expression fold change of ≥ 2 or ≤ 0.5 and an FDR $q \leq 0.05$ was applied to select the most differentially expressed genes. Intrinsic consensus molecular subtype (iCMS) assignment was performed using the R package CMScaller.(30) Gene Set Enrichment analysis (GSEA), Gene ontology pathway analysis and KEGG pathway analysis were performed using the GAGE(RRID:SCR_017067), clusterProfiler(v3.12, RRID:SCR_016884) and pathview(v3.12, RRID:SCR_002732) packages.(31-33)

Whole genome sequencing of DNA from organoids underwent short read whole genome sequencing (MGISEq) to a depth of 60x, outsourced to Nonacus Limited (Birmingham, UK). Reads were filtered and aligned to the GRCh38 genome and then underwent tumor:normal subtraction using Strelka2. Variant calls were annotated with VEP(v92, RRID:SCR_007931) and filtered to exclude any variant with a MAF >0.01 . A Boxplot was constructed for mutations from a merged MAF file using maftools.(34)

Nanopore long read sequencing including methylation calling was performed with library preparation of 1 μ g of DNA using the ONT LSK-109 kit (Oxford Nanopore Technologies, UK) according to manufacturer's protocol, and then loaded on an ONT Promethion R9.4.1 flowcell and run for 72 hours. FAST5 signal data was demultiplexed with Guppy 6(RRID:SCR_023196), FASTQ merged, trimmed with NanoFilt(RRID:SCR_016966) and aligned to the GRCh38 reference genome using MiniMap2(RRID:SCR_018550). Variant calling was performed with PEPPER-DeepVariant and Clair 3 using custom parameters to account for heterogenous cancer organoid samples. Structural variants were called using consensus

overlaps from cuteSV and Sniffles(RRID:SCR_017619). Copy number calling was performed using QDNASeq(RRID:SCR_003174) with 100kb bins and methylation calling was performed using Megalodon with a 5-methylcytosine model and output to BEDGraph files.

Bisulfite conversion and pyrosequencing

DNA underwent bisulfite conversion utilising the EZ DNA methylation kit (Zymo, USA). The sequence for the CpG island preceding CIITApIV (chr16:10,972,877-10,973,234 from UCSC; available from <https://genome.ucsc.edu/>) was input into the PyroMark Assay Design software (QIAGEN, version 2.0.2.5) and the following primers were obtained from Sigma-Aldrich (UK): *CIITA* Forward: 5'-GGGGGATGGAATATGTAAAATGTAG-3', *CIITA* Reverse-Biotin: 5'-CCCCCAAACCTAAACACAACAACC-3' and *CIITA* Sequencing: 5'-GGAATATGTAAAATGTAGGG-3'. PCR amplification of the region of interest was performed on bisulfite converted DNA using the PyroMark PCR kit (QIAGEN, Germany). Finally, pyrosequencing was performed in triplicate on a PyroMark Q48 sequencer using PyroMark Q48 Advanced Reagents (QIAGEN, Germany). Analysis of C/T ratio was performed by the PyroMark AutoPrep software.

Chromatin Immunoprecipitation (ChIP)

DNA was isolated from cells following treatment with 24 hours IFN γ stimulation or vehicle control. Single cross-linking of DNA with formaldehyde was performed for H3K9me2 and H3K9ac, with dual cross-linking (DSG/formaldehyde) performed for EZH2. Sonication and shearing of DNA was performed using a Covaris E220 Evolution and according to the truChIP Chromatin Shearing Kit (Covaris, USA) protocol. Overnight immunoprecipitation was performed with the following antibodies (Abcam, UK): H3K9ac (#ab4441, RRID:AB_2118292), H3K9me2 (#ab195482) and EZH2 (#ab195409). DNA was reversed cross-linked using Proteinase K (Roche, Germany) prior to purification with AMPure XP beads (Beckman Coulter, USA). Four PCR primers were used to cover the whole of CIITApIV as previously described.(2) PCR was performed using the PowerUp SYBR Green Master Mix (ThermoFisher Scientific, Lithuania) and related protocol, with an Applied Biosystems 7500 qPCR machine and determination of Ct values and melt-curve analysis performed using SDS software (Applied Biosystems). Quantification was performed relative to a genomic DNA standard curve and data from each region was normalised by input control.

TCGA analysis

Normalised Agilent microarray z-score data for EZH2 and all class II genes were extracted from The Cancer Genome Atlas (TCGA, RRID:SCR_003193) colorectal dataset using the cBioportal tool(RRID:SCR_014555).(35-37) Data were tabulated in Excel (Microsoft Corp.). Normality of distributions was confirmed with the Anderson-Darling test. Mean expression of all class II genes was calculated. Pearson Coefficient of determination (R and R²) values were calculated in Excel and Minitab (Minitab Inc, RRID:SCR_014483) to investigate correlations in gene expression.

Statistics

Statistical tests utilised are detailed alongside results and above, including unpaired T test, Fisher's exact and One-Way ANOVA with post-test (Tukey or Sidak) performed in GraphPad Prism (version 9.0.0, RRID:SCR_002798) and other analysis e.g. Wilcoxon rank-sum in Stata

16.1 (Statcorp, TX, RRID:SCR_012763) and Benjamini-Hochberg correction using R 4.1.0 (R Core Team, 2022, RRID:SCR_001905).

Data Availability

The data generated in this study are available within the article and its supplementary data files, with further raw data available upon request from the corresponding author. The genomic data have been deposited with links to BioProject accession number PRJNA978372 in the NCBI BioProject database (<https://www.ncbi.nlm.nih.gov/bioproject/>).

Results

Organoids were derived from 15 primary colorectal cancers. Seven were tsMHC-II negative by tissue immunohistochemistry (six of which were pMMR) and eight tsMHC-II positive (Table 1). Previous studies demonstrated that a proportion of CRC cell lines cannot be induced to express class II upon IFN γ treatment.(2) We first asked whether tsMHC-II negativity is due to a cell-autonomous lack of class II inducibility in response to IFN γ . Organoids and four cell lines with previously documented *CIIITA* promoter methylation status (HT29, DLD1, RKO and HCT116)(2) were treated with IFN γ and subsequent class II expression analysed by flow cytometry. Three types of response to 24 hours IFN γ stimulation were observed: strongly inducible (>50% cells expressing Class II), weakly inducible (10-49%) and non-inducible (<10%). (Figure 1a-f, Supplementary Figure 1).

Eight organoids demonstrated strong induction of class II expression by 24 hours (Table 1, Figure 1c,e), including 2 organoids derived from tsMHC-II negative cancers, assessed by class II IHC on the primary tumor slides. In four organoids (Figure 1b,d and Table 1) there was an intermediate pattern of class II inducibility with discernible but non-significant increases in class II expression at 24 hours of between 10-49% (weak subtype). Three of these weakly inducible organoids were tsMHC-II negative. In some fully class II inducible immortalised cell lines, full induction requires longer exposure to IFN γ .(38) We therefore exposed these four organoids to 72 hours of IFN γ . This resulted in high-level Class II induction in three of four of these organoids (81.4 - 94.9 % cells class II positive: Table 1, Figure 1g). Finally, three organoids displayed a complete absence of class II induction to IFN γ at both 24 and at 72 hours (Table 1, Figure 1a,d,g). All three were IHC tsMHC-II negative \leq 1%.

In CRC cell lines, non-inducibility has been attributed to *CIIITA* promoter methylation.(2) We analysed methylation at the *CIIITA*pIV promoter using bisulphite pyrosequencing in all 15 organoids and the four control CRC cell lines. Importantly, we found no evidence of methylation in any of the organoids including the three non-inducible organoids (Table 2). Two non-inducible cell lines previously identified as *CIIITA*pIV methylated (RKO and HCT116) were methylated as expected.(2) Based on the previously observed frequency (3/8) of 2D CRC cell lines demonstrating *CIIITA* methylation, this result of 0/15 organoids non-methylated is highly significant (probability-based $p=0.0009$; Fisher's exact $p=0.032$). Thus, *CIIITA* methylation is likely to be a 2D cell culture-mediated phenomenon and does not appear to be a relevant mechanism for silencing tsMHC-II in CRC.

As the non-inducible organoids had no evidence of *CIIITA* methylation, we asked whether IFN γ treatment was causing appropriate activation of the proximal IFN γ pathway.

Upregulation of STAT1 and IRF1 protein following IFN γ treatment was observed in all four of the control cell lines (Figure 2a) and all of the organoids with weak or strong class II inducibility (Figure 2c,d). However, in the three non-inducible organoids there was no change in STAT1 and IRF1 protein (Figure 2b) suggesting a defect in proximal signalling.

WGS was performed on all organoids. Mutational analysis demonstrated concordance with the primary tumor pathology analysis (Extended RAS and BRAF V600 clinical testing) and the observed organoid mutations (Figure 3a and Table 1). There was no evidence of *IFNGR* mutations in any of the organoids on whole genome sequencing. JAK1 is an obligatory molecule sub-serving downstream signalling from the IFN γ receptor and JAK1 loss is well described as an immunological escape mechanism in dMMR CRC(39) and as a resistance mechanism to checkpoint blockade in immunogenic cancers.(40) We performed RNAseq under basal (unstimulated) conditions to see if *JAK1*, *JAK2*, *JAK3* or IFN γ receptor message was differentially expressed in non-inducible versus inducible organoids. Following filtering, normalisation and variance stabilising transformation of all genes sequenced in this organoid dataset, 26474 genes were identified. Of these, 1269 genes were significantly ($p < 0.05$) differentially expressed between the inducible and non-inducible organoid groups (829 were upregulated in the inducible cohort and 440 were upregulated in the non-inducible cohort). *JAK1* expression was the third most significant differentially expressed gene in the entire sequenced transcriptome. *JAK1* had a positive log change of 2.862, indicating higher expression in the inducible cohort ($p = 1.21 \times 10^{-17}$ Benjamini-Hochberg correction) and was the gene most differentially down-regulated in the non-inducible group (Figure 3b). Gene set enrichment analysis and Gene Ontology analysis was performed (Supplementary Figure 2). Western blotting confirmed loss of JAK1 protein in the non-inducible organoids (Figure 2e).

Organoid CMS classification recapitulates typical CMS associations(41) and all three non-inducible organoids were MSI-like CMS1. All three contained highly deleterious mutations in the *JAK1* gene predicted to cause loss of function with two stop-gain mutations (organoid 376 *JAK1* GRCh38c.425insC p.142K/*; organoid 557 *JAK1* GRCh38c.2263C>T p.755R/*) and a 315bp insertion into an enhancer within intron 3 of organoid 964 at GRCh38:chr1:64881273 predicted to cause loss of function. *JAK1* mutation therefore likely provides a route of immune escape in this immunogenic CMS1 cohort.

Whole genome long-read nanopore sequencing also allows analysis of the methylation status of sequenced genes. Modified base calling of these organoids demonstrated consistent hypermethylation of the canonical *JAK1* promoter in the non-inducible organoids compared with inducible (median methylation 11.8% vs 0%, $p = 0.0011$) (Supplementary Figure 3). Although this difference is statistically significant, the degree of methylation was modest. The non-inducible organoids were therefore treated with azacitidine for up to 6 days before IFN γ exposure for up to 72 hours. However, no evidence of additional class II up-regulation after IFN γ (Supplementary Figure 4) was observed, in keeping with loss of function mutation in *JAK1* as the main barrier to JAK1 expression in this group.

Of the four weakly inducible organoids, one organoid (line 658), a dMMR BRAF-mutant line, failed to significantly upregulate class II expression even with 72 hours of IFN γ (Table 1, Figure 1g). To better understand *C/ITA* accessibility after 24 hours IFN γ stimulation across

this line and others, assessment of *CIITA* mRNA expression using RT-qPCR and *CIITA* occupancy/histone modification was performed using ChIP PCR. On RT-qPCR the non-inducible lines demonstrated the lowest relative increase of *CIITA* mRNA compared with the strong and weakly inducible organoids (Figure 4a), with 658 having the smallest increase with IFN γ stimulation in the inducible lines. Whilst the relative change in *CIITA* expression was similar between the weak and strong groups, the absolute levels of basal and IFN γ stimulated *CIITA* expression between the three response groups were significantly different (stimulated expression: Strong vs weak P=0.0004, Strong vs Negative P<0.0001, weak vs Negative P<0.0001, One-way ANOVA followed by Tukey's post-test)(Supplementary Table 2).

In highly metastatic breast cancer cell lines, an analogous subset is described demonstrating delayed class II upregulation following IFN γ exposure, mediated by IFN γ -induced EZH2 occupancy at *CIITA*.(38) We analysed EZH2 occupancy at *CIITA* using ChIP-PCR in the weakly inducible organoids and two fully inducible organoids (411 and 653) as controls. In the strongly inducible organoids, there was a decrease in EZH2-CIITA β occupancy as expected (411: 0.73-fold reduction p<0.001, 653: 0.35-fold reduction p<0.001). However, in line with the breast cancer data, all four weak lines demonstrated significant increases in EZH2 occupancy at *CIITA* with 24 hours IFN γ stimulation, with a particularly large increase observed in 658 (Figure 4b).

Dynamic changes in H3K9 acetylation (associated with chromatin accessibility) and H3K9 methylation (associated with transcriptional repression) following 24 hours IFN γ treatment were next assessed. In the strongly inducible lines and 658, there was a marked increase in *CIITA* H3K9 acetylation and no increase in H3K9 methylation (Figure 4c,d). In the remaining three weakly inducible organoids with low-level increases in IFN γ -mediated EZH2 occupancy at 24 hours, attenuated H3K9 acetylation was observed at 24 hours. Minimal change in either H3K9 acetylation or methylation was observed in the non-inducible lines, in keeping with loss of proximal pathway signalling. RKO (the methylated 2D cell line) was the only line to exhibit significantly increased H3K9 methylation following IFN γ , consistent with the promoter CpG methylation detected and as reported in the literature.(2) 658 had the smallest relative induction in *CIITA* mRNA after IFN γ (Figure 4a) of any of the inducible organoids, whilst still acquiring high levels of H3K9 acetylation and very high levels of EZH2 occupancy, suggesting a functional difference between this and the other organoids weakly inducible at 24 hours.

We assessed the relevance of EZH2 occupancy to the reduction or delay in tsMHC-II induction. 658 was treated with the EZH2 inhibitor GSK126 plus IFN γ which increased the number of cells positive from 12.6% at 72 hours with IFN γ alone to 24.9% (Figure 5). In the other organoids with delayed induction at 24 hours with IFN γ alone, there was also an approximate doubling of class II positive cells with GSK126/IFN γ co-treatment at 24 hours, the net effect being proportional to the amount of early induction with IFN γ alone (Figure 5). EZH2 occupancy-mediated H3K27 methylation and H3K27 acetylation are anti-correlated marks at *CIITA*.(38) *In vivo* HDAC1 and HDAC2 form a complex with EED/EZH2 and which has histone deacetylase activity and further EED-mediated gene repression involves histone deacetylation and can be reversed by HDAC inhibition.(42) Treatment with the class I HDAC inhibitor entinostat and IFN γ increased Class II expression to 65.1% of cancer cells at 72

hours in 658 and doubled the effect of GSK126 at 24 hours (Figure 5). Finally, using TCGA data we found an inverse correlation between EZH2 expression and mean class II expression ($R = -0.314$, $p=0.00017$) in pMMR CRC samples (Figure 6). Accompanying clinical characteristics provided by the Cancer Genome Atlas Network.(35)

Discussion

Using model *in vitro* systems that reproduce the promoter methylation of their tissue of origin,(24, 25) we show that providing IFN γ signalling is intact, the majority of colorectal cancer organoids are class II inducible. Furthermore, in all 15 organoids analysed there is no evidence of *CIITA* promoter methylation, contrary to the findings in 2D culture systems, which we have replicated herein as a positive control. There is further confirmatory evidence in CRC, with tissue microdissection from primary tissue samples failing to find any evidence of *CIITA* promoter methylation in twenty tsMHC-II negative tumors.(43) Together these findings in 3D and primary CRC samples confirm that *CIITA* methylation is not a biologically relevant route of immune evasion in CRC and is likely to be a culture-induced aberrant methylation pattern.(23)

6/8 strongly inducible organoids were tsMHC-II positive (on primary tumor IHC), two pMMR organoids, 080 and COLO312, had negative tsMHC-II on immunohistochemistry. Both of these had Immunoscore (IS)=2 suggesting that whilst T cells are present, they may be producing inadequate IFN γ , either because of lack of activation or functional suppression. The two other patterns of class II inducibility, absent and weakly inducible were largely associated with tsMHC-II negative cancers, with all pMMR cancers in these groups being tsMHC-II negative.

3/15 organoids showed loss of JAK1 expression with resultant non-responsiveness to IFN γ secondary to *JAK1* mutations. These three organoids were all MSI-like CMS1 consistent with enhanced immunogenicity which is associated with a stronger drive to evade immune surveillance. Although the three non-inducible organoids had low-level *JAK1* promoter methylation, this was not therapeutically tractable with azacitidine alone and loss of expression is much more likely to be a result of the deleterious *JAK1* mutations. JAK1 is a critical molecule linking IFN γ receptor activation to activation of all IFN γ -sensitive genes and loss of JAK1 downregulates class II, class I and CXCL9/10 in cancer cells. In immunogenic mouse models, cancer cell JAK1 loss abrogates the effect of dual checkpoint blockade and focal irradiation and inhibits the anti-tumor effect of adoptive transfer of antigen-specific T cells.(44) Loss of function mutations are well described as a cause of acquired resistance to checkpoint blockade in melanoma(40) and are seen in 17.8% dMMR CRC and 5.3% pMMR CRC.(39)

4/15 lines were weakly-inducible, however, only one of these lines (658) remained so following 72 hours IFN γ stimulation, the other three lines displaying eventual full induction with IFN γ and without the need for additional epigenetic therapies. In these four lines, high-level IFN γ -induced EZH2 occupancy at *CIITA* is observed as has previously been described, delaying and restricting Class II inducibility. Sustained 72-hour IFN γ exposure in the three 72-hour inducible organoids is presumably able to overcome the much more modest increase in EZH2-CIITA β occupancy compared to 658.(38)

We demonstrate a negative correlation between EZH2 and class II expression in CRC in the TCGA dataset, in addition to the negative correlation between EZH2 and CXCL9/10 previously described.(45) Our data adds to the evidence supporting a key role for EZH2 in repressing MHC expression. Small cell lung cancer (SCLC) has the lowest MHC-I expression of any cancer. EZH2 is highly expressed in SCLC, and EZH2 expression is negatively correlated with both MHC-I expression and CD8+ T cells in clinical samples.(46) EZH2 inhibition significantly reduced H3K27me3 levels and upregulated MHC-I and dramatically upregulated IFN γ -induced MHC-I expression. *In vivo* and *in vitro* EZH2 inhibition in bladder cancer significantly upregulates CIITA levels and tsMHC-II and the efficacy of therapy *in vivo* is wholly dependent on adaptive immunity. There is also an inverse correlation between EZH2 levels and immune-related transcripts in bladder cancer.(47)

It is clear from our data that using epigenetic modifiers to immunologically enhance the CRC microenvironment, specifically through their positive immunomodulatory effects of enhanced tsMHC-II expression, appears to be only appropriate in a minority of cancers (those of the weakly inducible sub-type). With regards to EZH2 inhibition, low concentrations of GSK126 enhance the growth of some CRC organoids,(48) an effect we confirm in a subset of the organoids in this dataset (Supplementary Figure 5). Aside from the promoting proliferation, there are additional adverse microenvironmental consequences seen with EZH2 inhibition that need to be considered carefully when utilizing these compounds clinically. Tumor infiltrating EZH2+ T cells are polyfunctional effectors resistant to apoptosis.(49) T cell activation increases EZH2 and treatment with GSK126 decreases the proportions of polyfunctional CD8+ T cells and increases T cell apoptosis. In a CRC model, GSK126 reduced the infiltration, proliferation and IFN γ production of CD8+ T cells, mediated by increased MDSCs.(50)

Class I HDAC inhibitors, such as entinostat, have potent anti-MDSC effects *in vivo*(51, 52) and entinostat alone significantly upregulates IFN γ -induced Class II expression in line 658 in keeping with its role in EED-mediated gene repression.(42) Mocetinostat, another class I HDAC inhibitor, also significantly augments CIITA expression and class II protein expression in response to IFN γ .(53) However, as with EZH2 inhibition, HDAC inhibitors also have negative microenvironmental effects, particularly on DCs, already present at low levels in CRC.(54, 55) Attempts to modulate the TME with epigenetic therapies must take into account the negative microenvironmental consequences of epigenetic therapies. Finally, whilst *CIITA* promoter methylation appears not to be an important mechanism of tsMHC-II loss in CRC, multiple other immune-related genes may be repressed by promoter methylation, including endogenous retroviral genes and thus the combination of DNMT inhibitors with checkpoint blockade has been studied. In the phase II trial of azacitidine plus pembrolizumab in pMMR CRC, response rate was only 3% with median PFS 1.9 months despite evidence of global DNA demethylation.(56) Additionally, the combination of 5-azacitidine and pembrolizumab *plus* the addition of the HDAC inhibitor romidepsin has minimal activity in pMMR CRC.(57)

A potential limitation is that the data herein was generated *in vitro*. However, we specifically wanted to explore the cell-autonomous mechanisms of class II regulation in epigenetically relevant human models. In addition, we have not examined whether upregulated tsMHC-II expression can present antigen in an efficacious manner to CD4+ T

cells, as the remit of this work was specifically to interrogate the dynamics of class II expression itself, given the previous cell line data suggesting *CIITA* methylation as an immune evasion mechanism. However, earlier data has shown that CRC cells treated with IFN γ can indeed take up, process and present intact antigen in an HLA-DR restricted manner(12) and immunological protection of *CIITA* transfected is due to the generation of primed CD4+ T cells providing help for the generation of cancer antigen-specific cytotoxic T cell effectors.(7, 10) The relatively limited number of organoids is another limitation, but the three inducibility phenotypes described herein appear discrete and robust and we continue to derive primary colorectal organoids to elucidate if there are further rare patterns of tsMHC-II inducibility. Furthermore, we have shown that given the number analysed, our finding of 0/15 organoids with methylated *CIITA*, compared with previous expectations from cell line data is significant and is supported by data from primary samples.(43)

In conclusion, we provide an analysis of the patterns and dynamics of class II induction in CRC and the epigenetic marks that underlie them, using an *in vitro* PDO model system and IFN γ , the crucial microenvironmental cytokine. This data demonstrates the individual variation in these dynamics and their epigenetic associations and may explain the difficulty in translating epigenetic modifiers to specifically augment tsMHC-II inducibility. This approach can serve as a blueprint for investigating the heterogeneity of specific epigenetic mechanisms of immune suppression across individual patients in other cancers and how these might be targeted to inform the conduct of future trials of epigenetic therapies as immune adjuvants more strategically in cancer.

References:

1. Lovig T, Andersen SN, Thorstensen L, Diep CB, Meling GI, Lothe RA, et al. Strong HLA-DR expression in microsatellite stable carcinomas of the large bowel is associated with good prognosis. *Br J Cancer*. 2002;87(7):756-62.
2. Satoh A, Toyota M, Ikeda H, Morimoto Y, Akino K, Mita H, et al. Epigenetic inactivation of class II transactivator (CIITA) is associated with the absence of interferon-gamma-induced HLA-DR expression in colorectal and gastric cancer cells. *Oncogene*. 2004;23(55):8876-86.
3. Londhe P, Zhu B, Abraham J, Keller C, Davie J. CIITA is silenced by epigenetic mechanisms that prevent the recruitment of transactivating factors in rhabdomyosarcoma cells. *Int J Cancer*. 2012;131(4):E437-48.
4. Holling TM, Bergevoet MW, Wilson L, Van Eggermond MC, Schooten E, Steenbergen RD, et al. A role for EZH2 in silencing of IFN-gamma inducible MHC2TA transcription in uveal melanoma. *J Immunol*. 2007;179(8):5317-25.
5. van der Stoep N, Biesta P, Quinten E, van den Elsen PJ. Lack of IFN-gamma-mediated induction of the class II transactivator (CIITA) through promoter methylation is predominantly found in developmental tumor cell lines. *Int J Cancer*. 2002;97(4):501-7.
6. Meazza R, Comes A, Orengo AM, Ferrini S, Accolla RS. Tumor rejection by gene transfer of the MHC class II transactivator in murine mammary adenocarcinoma cells. *Eur J Immunol*. 2003;33(5):1183-92.

7. Mortara L, Castellani P, Meazza R, Tosi G, De Lerma Barbaro A, Procopio FA, et al. CIITA-induced MHC class II expression in mammary adenocarcinoma leads to a Th1 polarization of the tumor microenvironment, tumor rejection, and specific antitumor memory. *Clin Cancer Res.* 2006;12(11 Pt 1):3435-43.
8. Bou Nasser Eddine F, Forlani G, Lombardo L, Tedeschi A, Tosi G, Accolla RS. CIITA-driven MHC class II expressing tumor cells can efficiently prime naive CD4(+) TH cells in vivo and vaccinate the host against parental MHC-II-negative tumor cells. *Oncoimmunology.* 2017;6(1):e1261777.
9. Borst J, Ahrends T, Bąbata N, Melief CJM, Kastenmüller W. CD4(+) T cell help in cancer immunology and immunotherapy. *Nat Rev Immunol.* 2018;18(10):635-47.
10. Mortara L, Frangione V, Castellani P, De Lerma Barbaro A, Accolla RS. Irradiated CIITA-positive mammary adenocarcinoma cells act as a potent anti-tumor-preventive vaccine by inducing tumor-specific CD4+ T cell priming and CD8+ T cell effector functions. *Int Immunol.* 2009;21(6):655-65.
11. Telega GW, Baumgart DC, Carding SR. Uptake and presentation of antigen to T cells by primary colonic epithelial cells in normal and diseased states. *Gastroenterology.* 2000;119(6):1548-59.
12. Hershberg RM, Framson PE, Cho DH, Lee LY, Kovats S, Beitz J, et al. Intestinal epithelial cells use two distinct pathways for HLA class II antigen processing. *J Clin Invest.* 1997;100(1):204-15.
13. Accolla RS, Ramia E, Tedeschi A, Forlani G. CIITA-Driven MHC Class II Expressing Tumor Cells as Antigen Presenting Cell Performers: Toward the Construction of an Optimal Anti-tumor Vaccine. *Front Immunol.* 2019;10:1806.
14. Johnson AM, Bullock BL, Neuwelt AJ, Poczobutt JM, Kaspar RE, Li HY, et al. Cancer Cell-Intrinsic Expression of MHC Class II Regulates the Immune Microenvironment and Response to Anti-PD-1 Therapy in Lung Adenocarcinoma. *J Immunol.* 2020;204(8):2295-307.
15. Oh DY, Kwek SS, Raju SS, Li T, McCarthy E, Chow E, et al. Intratumoral CD4(+) T Cells Mediate Anti-tumor Cytotoxicity in Human Bladder Cancer. *Cell.* 2020;181(7):1612-25.e13.
16. Cachot A, Bilous M, Liu YC, Li X, Saillard M, Cenerenti M, et al. Tumor-specific cytolytic CD4 T cells mediate immunity against human cancer. *Sci Adv.* 2021;7(9).
17. Böttcher JP, Bonavita E, Chakravarty P, Blees H, Cabeza-Cabrerizo M, Sammicheli S, et al. NK Cells Stimulate Recruitment of cDC1 into the Tumor Microenvironment Promoting Cancer Immune Control. *Cell.* 2018;172(5):1022-37.e14.
18. Clevers H, Nusse R. Wnt/ β -catenin signaling and disease. *Cell.* 2012;149(6):1192-205.
19. Spranger S, Bao R, Gajewski TF. Melanoma-intrinsic beta-catenin signalling prevents anti-tumour immunity. *Nature.* 2015;523(7559):231-5.
20. Ferris ST, Durai V, Wu R, Theisen DJ, Ward JP, Bern MD, et al. cDC1 prime and are licensed by CD4(+) T cells to induce anti-tumour immunity. *Nature.* 2020;584(7822):624-9.
21. Fahrner JA, Eguchi S, Herman JG, Baylin SB. Dependence of histone modifications and gene expression on DNA hypermethylation in cancer. *Cancer Res.* 2002;62(24):7213-8.
22. Smiraglia DJ, Rush LJ, Fruhwald MC, Dai Z, Held WA, Costello JF, et al. Excessive CpG island hypermethylation in cancer cell lines versus primary human malignancies. *Hum Mol Genet.* 2001;10(13):1413-9.
23. Suter CM, Norrie M, Ku SL, Cheong KF, Tomlinson I, Ward RL. CpG island methylation is a common finding in colorectal cancer cell lines. *Br J Cancer.* 2003;88(3):413-9.

24. Kraiczy J, Nayak KM, Howell KJ, Ross A, Forbester J, Salvestrini C, et al. DNA methylation defines regional identity of human intestinal epithelial organoids and undergoes dynamic changes during development. *Gut*. 2019;68(1):49-61.
25. Wang R, Mao Y, Wang W, Zhou X, Wang W, Gao S, et al. Systematic evaluation of colorectal cancer organoid system by single-cell RNA-Seq analysis. *Genome Biol*. 2022;23(1):106.
26. Garris CS, Arlauckas SP, Kohler RH, Trefny MP, Garren S, Piot C, et al. Successful Anti-PD-1 Cancer Immunotherapy Requires T Cell-Dendritic Cell Crosstalk Involving the Cytokines IFN- γ and IL-12. *Immunity*. 2018;49(6):1148-61.e7.
27. Sato T, Stange DE, Ferrante M, Vries RG, Van Es JH, Van den Brink S, et al. Long-term expansion of epithelial organoids from human colon, adenoma, adenocarcinoma, and Barrett's epithelium. *Gastroenterology*. 2011;141(5):1762-72.
28. van de Wetering M, Francies HE, Francis JM, Bounova G, Iorio F, Pronk A, et al. Prospective derivation of a living organoid biobank of colorectal cancer patients. *Cell*. 2015;161(4):933-45.
29. Ahmed D, Eide PW, Eilertsen IA, Danielsen SA, Eknaes M, Hektoen M, et al. Epigenetic and genetic features of 24 colon cancer cell lines. *Oncogenesis*. 2013;2:e71.
30. Eide PW, Bruun J, Lothe RA, Sveen A. CMScaller: an R package for consensus molecular subtyping of colorectal cancer pre-clinical models. *Sci Rep*. 2017;7(1):16618.
31. Luo W, Brouwer C. Pathview: an R/Bioconductor package for pathway-based data integration and visualization. *Bioinformatics*. 2013;29(14):1830-1.
32. Luo W, Friedman MS, Shedden K, Hankenson KD, Woolf PJ. GAGE: generally applicable gene set enrichment for pathway analysis. *BMC Bioinformatics*. 2009;10:161.
33. Yu G, Wang LG, Han Y, He QY. clusterProfiler: an R package for comparing biological themes among gene clusters. *OMICS*. 2012;16(5):284-7.
34. Mayakonda A, Lin DC, Assenov Y, Plass C, Koeffler HP. Maftools: efficient and comprehensive analysis of somatic variants in cancer. *Genome Res*. 2018;28(11):1747-56.
35. Cancer Genome Atlas Network. Comprehensive molecular characterization of human colon and rectal cancer. *Nature*. 2012;487(7407):330-7.
36. Gao J, Aksoy BA, Dogrusoz U, Dresdner G, Gross B, Sumer SO, et al. Integrative analysis of complex cancer genomics and clinical profiles using the cBioPortal. *Sci Signal*. 2013;6(269):p11.
37. Cerami E, Gao J, Dogrusoz U, Gross BE, Sumer SO, Aksoy BA, et al. The cBio cancer genomics portal: an open platform for exploring multidimensional cancer genomics data. *Cancer Discov*. 2012;2(5):401-4.
38. Truax AD, Thakkar M, Greer SF. Dysregulated recruitment of the histone methyltransferase EZH2 to the class II transactivator (CIITA) promoter IV in breast cancer cells. *PLoS One*. 2012;7(4):e36013.
39. Albacker LA, Wu J, Smith P, Warmuth M, Stephens PJ, Zhu P, et al. Loss of function JAK1 mutations occur at high frequency in cancers with microsatellite instability and are suggestive of immune evasion. *PLoS One*. 2017;12(11):e0176181.
40. Zaretsky JM, Garcia-Diaz A, Shin DS, Escuin-Ordinas H, Hugo W, Hu-Lieskovan S, et al. Mutations Associated with Acquired Resistance to PD-1 Blockade in Melanoma. *N Engl J Med*. 2016;375(9):819-29.
41. Sveen A, Bruun J, Eide PW, Eilertsen IA, Ramirez L, Murumägi A, et al. Colorectal Cancer Consensus Molecular Subtypes Translated to Preclinical Models Uncover Potentially Targetable Cancer Cell Dependencies. *Clin Cancer Res*. 2018;24(4):794-806.

42. van der Vlag J, Otte AP. Transcriptional repression mediated by the human polycomb-group protein EED involves histone deacetylation. *Nat Genet.* 1999;23(4):474-8.
43. Michel S, Linnebacher M, Alcaniz J, Voss M, Wagner R, Dippold W, et al. Lack of HLA class II antigen expression in microsatellite unstable colorectal carcinomas is caused by mutations in HLA class II regulatory genes. *Int J Cancer.* 2010;127(4):889-98.
44. Kalbasi A, Tariveranmoshabad M, Hakimi K, Kremer S, Campbell KM, Funes JM, et al. Uncoupling interferon signaling and antigen presentation to overcome immunotherapy resistance due to JAK1 loss in melanoma. *Sci Transl Med.* 2020;12(565).
45. Nagarsheth N, Peng D, Kryczek I, Wu K, Li W, Zhao E, et al. PRC2 Epigenetically Silences Th1-Type Chemokines to Suppress Effector T-Cell Trafficking in Colon Cancer. *Cancer Res.* 2016;76(2):275-82.
46. Burr ML, Sparbier CE, Chan KL, Chan YC, Kersbergen A, Lam EYN, et al. An Evolutionarily Conserved Function of Polycomb Silences the MHC Class I Antigen Presentation Pathway and Enables Immune Evasion in Cancer. *Cancer Cell.* 2019;36(4):385-401.e8.
47. Piunti A, Meghani K, Yu Y, Robertson AG, Podojil JR, McLaughlin KA, et al. Immune activation is essential for the antitumor activity of EZH2 inhibition in urothelial carcinoma. *Sci Adv.* 2022;8(40):eabo8043.
48. Koppens MA, Bounova G, Cornelissen-Steijger P, de Vries N, Sansom OJ, Wessels LF, et al. Large variety in a panel of human colon cancer organoids in response to EZH2 inhibition. *Oncotarget.* 2016;7(43):69816-28.
49. Zhao E, Maj T, Kryczek I, Li W, Wu K, Zhao L, et al. Cancer mediates effector T cell dysfunction by targeting microRNAs and EZH2 via glycolysis restriction. *Nat Immunol.* 2016;17(1):95-103.
50. Huang S, Wang Z, Zhou J, Huang J, Zhou L, Luo J, et al. EZH2 Inhibitor GSK126 Suppresses Antitumor Immunity by Driving Production of Myeloid-Derived Suppressor Cells. *Cancer Res.* 2019;79(8):2009-20.
51. Kim K, Skora AD, Li Z, Liu Q, Tam AJ, Blosser RL, et al. Eradication of metastatic mouse cancers resistant to immune checkpoint blockade by suppression of myeloid-derived cells. *Proc Natl Acad Sci U S A.* 2014;111(32):11774-9.
52. Orillion A, Hashimoto A, Damayanti N, Shen L, Adelaiye-Ogala R, Arisa S, et al. Entinostat Neutralizes Myeloid-Derived Suppressor Cells and Enhances the Antitumor Effect of PD-1 Inhibition in Murine Models of Lung and Renal Cell Carcinoma. *Clin Cancer Res.* 2017;23(17):5187-201.
53. Briere D, Sudhakar N, Woods DM, Hallin J, Engstrom LD, Aranda R, et al. The class I/IV HDAC inhibitor mocetinostat increases tumor antigen presentation, decreases immune suppressive cell types and augments checkpoint inhibitor therapy. *Cancer Immunol Immunother.* 2018;67(3):381-92.
54. Nencioni A, Beck J, Werth D, Grünebach F, Patrone F, Ballestrero A, et al. Histone deacetylase inhibitors affect dendritic cell differentiation and immunogenicity. *Clin Cancer Res.* 2007;13(13):3933-41.
55. Brogdon JL, Xu Y, Szabo SJ, An S, Buxton F, Cohen D, et al. Histone deacetylase activities are required for innate immune cell control of Th1 but not Th2 effector cell function. *Blood.* 2007;109(3):1123-30.
56. Kuang C, Park Y, Augustin RC, Lin Y, Hartman DJ, Seigh L, et al. Pembrolizumab plus azacitidine in patients with chemotherapy refractory metastatic colorectal cancer: a single-arm phase 2 trial and correlative biomarker analysis. *Clin Epigenetics.* 2022;14(1):3.

57. Baretta M, Murphy AG, Zahurak M, Gianino N, Parkinson R, Walker R, et al. A study of using epigenetic modulators to enhance response to pembrolizumab (MK-3475) in microsatellite stable advanced colorectal cancer. *Clin Epigenetics*. 2023;15(1):74.

Organoid Line	Negative			Weak				Strong							
	376	557	964	389	658	884	COLO312	064	080	157	411	647	653	COLO151	COLO155
Class II Primary IHC (%)	0	1	0	0	20	0	0	25	0	45	1.5	75	60	0	7.5
24hr Flow Class II (% cells)	3.32	3.23	2.67	28.2	13.7	18.4	42.7	69.4	72.5	73.0	76.6	69.8	78.9	72.9	87.5
72hr Flow Class II (% cells)	5.54	1.31	0.21	85.1	11.9	75.9	82.0	n/a	n/a	n/a	n/a	n/a	n/a	n/a	n/a
Class I	+/-	+	-	+	+	+	+	+	+	-	+	-	+	+	+
Immunoscore	n/a	2	2	0	n/a	0	n/a	3	2	4	2	n/a	2	2	2
Immunoscore group	n/a	Int	Int	Low	n/a	Low	n/a	High	Int	High	Int	n/a	Int	Int	Int
CMS	1	1	1	2	n/a	2	1	2	2	1	3	4	4	3	4
Sex	M	F	M	M	F	M	F	M	F	F	F	M	F	M	M
Age at Diagnosis	51	75	53	81	59	74	n/a	79	85	84	74	45	55	71	60
Left/Right sided primary	L	R	R	R	R	L	R	L	L	R	R	R	L	R	L
Stage	II	II	I	III	II	IV	II	III	II	III	IV	III	I	III	II
Grade	Poor	Poor	Mod	Mod	Poor	Poor	Poor	Mod	Mod	Poor	Mod	Poor	Mod	Mod	Mod
RAS	n/a	KRAS	n/a	-	-	NRAS	KRAS	-	n/a	n/a	-	KRAS	KRAS	-	KRAS
BRAF	n/a	-	n/a	-	V600	-	-	-	n/a	-	V600	-	-	V600	-
MMR	pMMR	dMMR	pMMR	pMMR	dMMR	pMMR	dMMR	pMMR	pMMR	dMMR	pMMR	dMMR	pMMR	pMMR	pMMR

Table 1 Clinicopathological characteristics of organoids and MHC expression. Organoids grouped by mean 24 hour and 72 hour Class II expression as assessed by flow cytometry following IFN γ stimulation. MHC Class I status (flow cytometry) as present (+), weak (+/-) or absent (-). Relevant clinical correlates including Mean Class II expression (percentage positive cells) performed by IHC on primary tumour sections, Immunoscore (for eleven samples, four technical fails by provider) including score and group (Low, Intermediate, High), Consensus Molecular Subtype (CMS; as determined by CMScaller, one line 'indeterminant'), sex, age, side of primary, TNM stage and break-down, grade and extended RAS, BRAF and mismatch repair status (proficient pMMR vs deficient dMMR) as determined by clinical pathology service.

Line	CpG Methylation % (Standard Deviation)								All
	CpG 1	CpG 2	CpG 3	CpG 4	CpG 5	CpG 6	CpG 7	CpG 8	
HT29	3.2 (1.2)	2.6 (0.4)	5.5 (0.4)	4.9 (0.3)	5.1 (0.2)	2.4 (0.7)	3.3 (1.3)	3.2 (1.4)	3.8 (0.4)
DLD1	6.0 (1.7)	7.1 (1.6)	12.9 (0.7)	9.1 (0.5)	13.1 (0.2)	5.4 (0.9)	5.6 (0.3)	4.9 (1.0)	8.0 (0.2)
RKO	13.0 (0.7)	15.7 (1.2)	49.9 (3.3)	44.5 (1.3)	42.3 (2.1)	37.4 (0.4)	15.1 (0.6)	16.6 (0.4)	29.3 (0.8)
HCT116	59.9 (11.0)	65.0 (5.8)	96.8 (5.5)	83.8 (1.0)	74.1 (4.1)	79.8 (1.3)	100.0 (0.0)	94.7 (2.4)	81.8 (2.7)
376	2.3 (0.7)	2.5 (0.3)	1.8 (0.4)	0.9 (0.2)	1.0 (0.1)	0.8 (0.3)	1.1 (0.3)	1.1 (0.2)	1.4 (0.2)
557	3.4 (1.1)	3.0 (0.7)	3.2 (0.4)	1.8 (0.5)	2.6 (0.7)	1.9 (1.1)	2.7 (1.6)	2.5 (1.2)	2.6 (0.7)
964	3.7 (0.6)	3.5 (1.0)	4.5 (0.5)	3.1 (0.7)	6.9 (0.5)	2.8 (1.2)	3.1 (1.5)	2.3 (1.1)	3.7 (0.8)
389	2.8 (0.7)	2.9 (0.9)	3.2 (0.7)	1.7 (0.4)	2.2 (1.1)	1.6 (0.8)	2.3 (1.2)	2.6 (1.5)	2.4 (0.6)
658	3.1 (0.7)	3.2 (1.2)	6.3 (0.4)	5.5 (0.6)	12.7 (0.8)	2.9 (0.1)	3.7 (0.8)	3.5 (1.2)	5.1 (0.3)
884	3.1 (0.4)	2.4 (0.8)	2.5 (0.3)	1.4 (0.4)	1.8 (0.9)	1.8 (1.1)	2.2 (1.2)	2.2 (1.3)	2.2 (0.5)
COLO312	3.4 (0.6)	4.4 (0.7)	11.0 (0.3)	3.0 (0.4)	3.5 (0.2)	1.2 (0.3)	1.7 (0.4)	1.9 (0.3)	3.8 (0.3)
064	2.9 (0.5)	3.7 (0.7)	4.8 (0.7)	3.0 (0.4)	4.3 (0.6)	2.8 (1.2)	3.8 (1.6)	2.7 (1.3)	3.5 (0.8)
080	2.9 (0.9)	2.6 (0.6)	3.2 (0.3)	1.6 (0.3)	5.0 (0.7)	2.4 (1.4)	2.4 (1.1)	2.0 (1.2)	2.8 (0.5)
157	2.1 (1.0)	2.4 (0.7)	3.4 (0.4)	1.6 (0.4)	1.5 (0.6)	1.5 (0.9)	1.9 (1.1)	2.3 (1.5)	2.1 (0.4)
411	3.0 (0.5)	3.3 (0.4)	3.6 (0.5)	2.7 (0.1)	3.8 (1.0)	2.0 (1.3)	3.0 (1.6)	3.3 (1.1)	3.1 (0.6)
647	3.0 (0.6)	2.9 (0.7)	2.8 (1.0)	1.3 (0.4)	1.8 (0.2)	1.1 (0.0)	1.3 (0.3)	1.7 (0.5)	2.0 (0.4)
653	3.3 (0.5)	2.8 (0.6)	2.9 (0.6)	1.8 (0.9)	1.9 (1.2)	1.9 (1.4)	2.6 (1.4)	2.1 (1.5)	2.4 (1.0)
COLO151	2.6 (1.4)	2.8 (0.6)	3.3 (0.9)	1.7 (0.7)	1.8 (0.4)	1.7 (1.1)	2.3 (1.3)	2.7 (1.9)	2.4 (0.6)
COLO155	2.2 (1.0)	2.7 (0.5)	2.9 (0.8)	1.3 (0.8)	1.8 (0.9)	1.3 (0.8)	1.8 (1.0)	1.9 (1.3)	2.0 (0.6)

Table 2 Pyrosequencing results for CIITApIV methylation. Cell line and organoid (grouped by non-, weak- and strong- responses to IFN γ) DNA was bisulfite converted prior to PCR and determination of CpG methylation status of CIITApIV using pyrosequencing. All experiments performed in triplicate. Results displayed show the mean methylation percentage at each CpG site and standard deviation of data. The final column is a mean value across all CpG sites in that sample

Figure Legends

Figure 1 Class II inducibility across cell line and colorectal cancer organoids following IFN γ stimulation.

A-C Flow cytometry assessment of Class I and II expression across lines reveal three groups of response to stimulation at 24 hours (A-C). Representative plots, with two lines displayed for each group, for non-inducible (<10% Class II expression, A), weakly-inducible (10-49%, B) and strongly-inducible lines (>50%, C). Histogram overlay, right panel, for Class II expression between control (red) and IFN γ (blue). Flow data from all 15 organoids available in **Supplementary Figure 1**. **D-F** Class II expression following 24 hours stimulation for all lines, performed in minimum of triplicate, unpaired T test (NS $P \geq 0.05$; * $P < 0.05$; ** $P < 0.01$; *** $P < 0.001$). Lines grouped into non/weakly inducible (D), strongly inducible (E) and cell lines (F). **G** 72 hour stimulation of weakly- and non-inducible lines, results in triplicate and statistics as above. **H** Flow cytometry gating strategy.

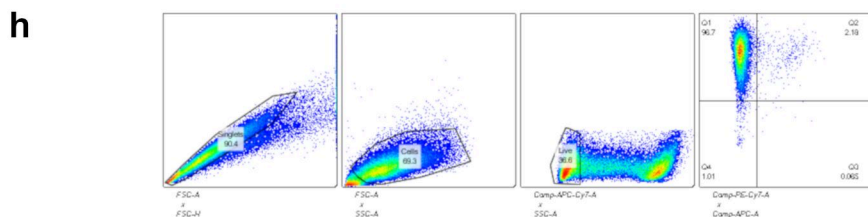
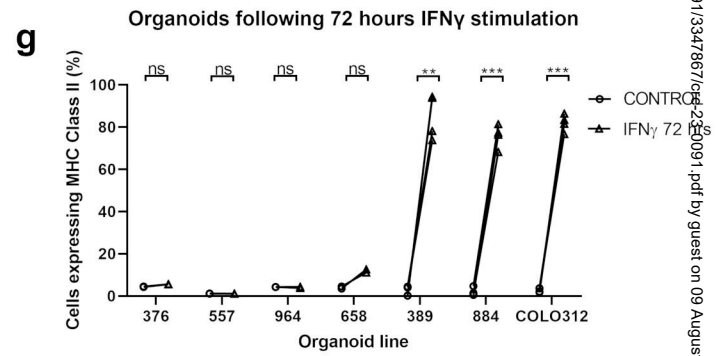
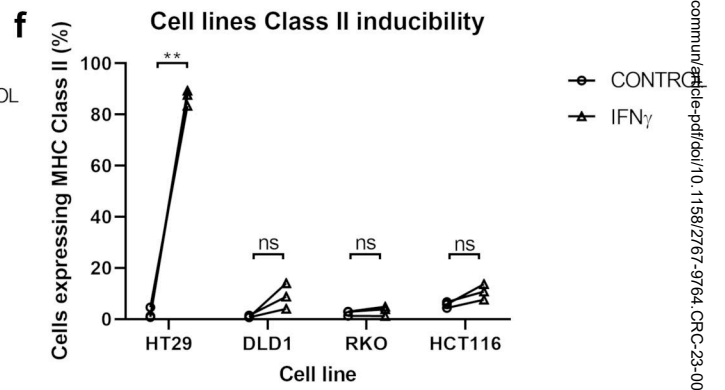
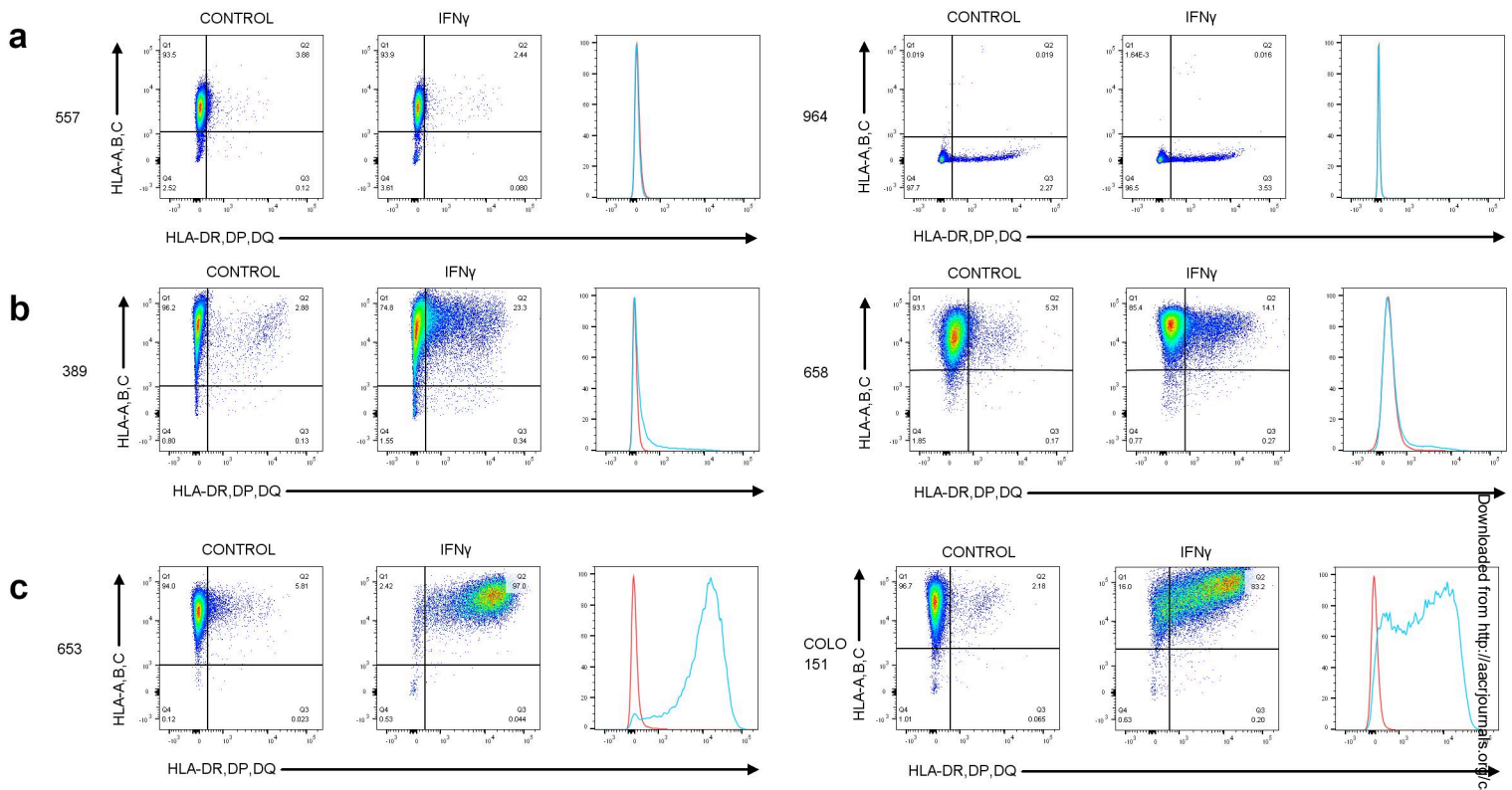
Figure 2 Western blot for IFN γ signalling pathway component integrity. A-D IFN γ responsiveness assessed with STAT1 and IRF1 following 24 hours stimulation demonstrating appropriate increases in protein in all cell lines (A), weakly (C) and strongly inducible (D) organoids. Loss of signalling response is noted in the non-inducible lines (B). **E** All organoid lines and A549, a control cell line with known JAK1 expression were assessed for JAK1 expression under basal conditions, with loss of protein expression confirmed in the non-inducible lines. Representative blots following triplicate experiments displayed.

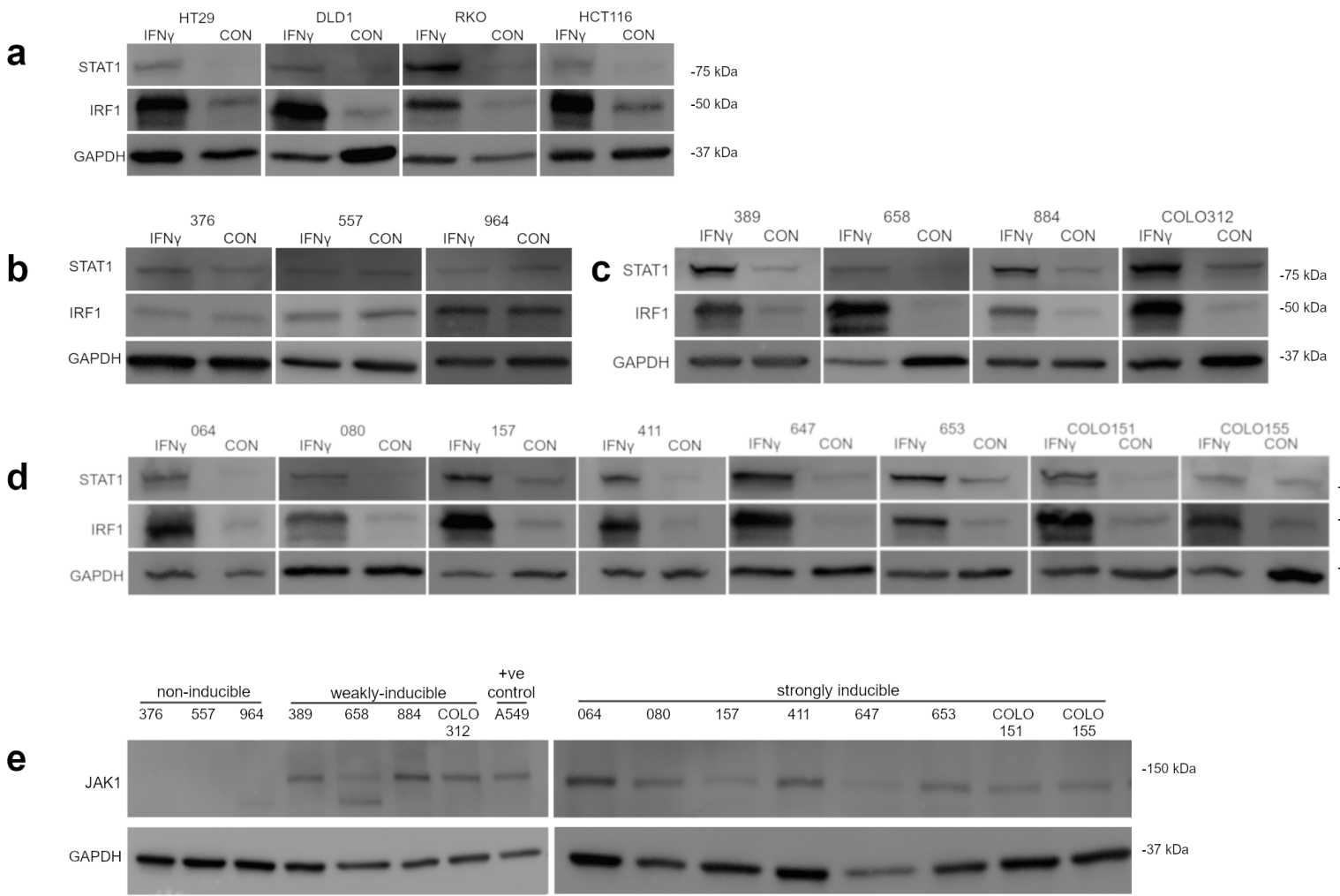
Figure 3 Genomic assessment of organoids. A Tile plot of common mutations on WGS of organoid cultures, created with Maftools. **B** Volcano plot for differential gene expression (RNAseq, unstimulated organoids) between inducible and non-inducible lines, most significant genes annotated including *JAK1*. Positive change upregulated in inducible lines.

Figure 4 CIITA accessibility and expression following IFN γ stimulation. A RT-qPCR for change in CIITA mRNA expression following stimulation across the organoid lines. Results divided by response groups (dotted lines) Calculated mean expression change and standard deviation displayed, with four technical replicates for each line. Note logarithmic scale on y-axis. Statistics applied across response groups (see main text) for biological replication. **B** ChIP PCR for EZH2 occupancy of the CIITA promoter, mean change across the four regions of the CIITA-pIV, controlled for input DNA, given for the weakly-inducible lines and two representative strongly inducible lines. Results performed with four replicates, with mean and SEM plotted. **C-D** ChIP PCR for change in CIITA-pIV H3K9ac (C) and H3K9me2 (D), again displaying mean across the four regions of CIITA-pIV controlled for input DNA. All organoid lines and an example inducible (HT29) and non-inducible (RKO) cell line treated. Horizontal line to demonstrate no change (relative change of 1). Results performed in triplicate with mean and SEM plotted. Statistics (unpaired T test) displayed for significant results * $P < 0.05$; ** $P < 0.01$; *** $P < 0.001$

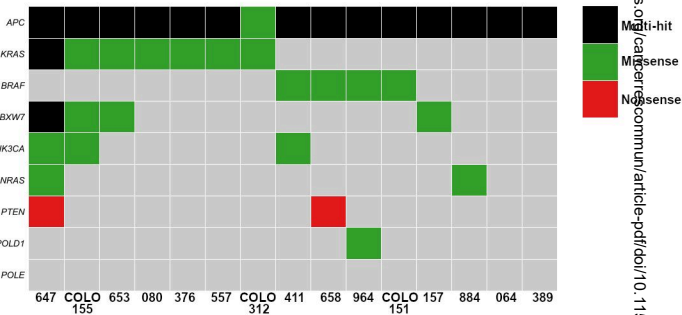
Figure 5 Pharmaceutical enhancement of Class II inducibility in weakly inducible organoids. Weakly inducible lines were stimulated for 24 and 72 hours and additionally treated with 2 μ M GSK126 (EZH2 inhibitor) for six days +/- 5 μ M Entinostat (HDAC inhibitor) for 72 hours. Flow cytometry data (mean Class II expression and SD) displayed from experiments performed in triplicate. Statistical analysis (One-way ANOVA followed by Sidak's post-test) performed for the addition of GSK126. NS $P \geq 0.05$; * $P < 0.05$; ** $P < 0.01$; *** $P < 0.001$; **** $P < 0.0001$. The addition of Entinostat was relatively toxic with relatively few viable events and therefore statistics have not been applied.

Figure 6 TCGA data on EZH2 and MHC Class II expression. Inverse correlation ($R = -0.314$, $p=0.00017$ Pearson correlation coefficient) of EZH2 and MHC Class II expression derived from the pMMR colorectal cancer dataset. 140 patients all derived from primary tumours. Characteristics: 43.6% female, 74.3% rectal/left-sided, 28.6% Stage III/15.% Stage IV, 53.6% RAS mutant, 4.3% BRAF mutant.





a



b

